SAE INTERNATIONAL

2023-24-0181

Published: August 28, 2023

HIL based real-time co-simulation for BEV fault injection testing

Anja Konzept[1], Benedikt Reick[1], Igor Pintaric[2] and Caio Osorio[2]

[1]Ravensburg-Weingarten University

[2]Typhoon HIL

Citation: Konzept, A., Reick, B., Pintaric, I., and Osório, C., "HIL based Real-Time Co-Simulation for BEV Fault Injection Testing," SAE Technical Paper 2023-24-0181, 2023, doi:10.4271/2023-24-0181.

DOI: https://doi.org/10.4271/2023-24-0181

Received: 13 May 2023 Revised: 29 Jun 2023 Accepted: 3 Jul 2023

Abstract

Battery electric vehicle (BEV) adoption and complex powertrains pose new challenges to automotive industries, requiring comprehensive testing and validation strategies for reliability and safety. Hardware-in-the-loop (HIL) based real-time simulation is important, with cooperative simulation (co-simulation) being an effective way to verify system functionality across domains. Fault injection testing (FIT) is crucial for standards like ISO 26262. This study proposes a HIL-based real-time co-simulation environment that enables fault injection tests in BEVs to allow evaluation of their effects on the safety of the vehicle. A Typhoon HIL system is used in combination with the IPG CarMaker environment. A four-wheel drive BEV model is built, considering high-fidelity electrical models of the powertrain components (inverter, electric machine, traction battery) and the battery management system (BMS). Additionally, it enables validation of driving dynamics, routes and environmental influences and provides a precise analysis of the effect of powertrain system faults on driving behavior. A possible case for a fault injection is to introduce a shoot-through fault in the inverter. Through the co-simulation, it is possible to analyze the effects on the powertrain and the vehicle dynamics in different driving situations (e.g. snow). This work demonstrates that co-simulation is a valuable tool for the development and validation of BEVs, and presents specific fault cases introduced into the powertrain and the resulting effects tested under different driving conditions. In addition, the study discusses the system's limitations and future possibilities such as controller hardware integration (Controller-HIL) and autonomous driving system validation.

Introduction

The development of electric propulsion systems for vehicles has made significant progress in recent years due to the increasing demand for low-emission vehicles. However, the increasing complexity of vehicles presents a major challenge for developers. The development of these propulsion systems is associated with a variety of challenges, such as ensuring system quality and validating systems, while also striving for fast and cost-effective development. To meet these challenges, simulation is used as an important tool in the development of electric vehicles [1, 2].

HIL real-time simulation is a testing technique that can be employed in the development of electric powertrain systems. This approach allows the simulation of electric powertrain systems under real-world conditions by emulating its electric components in a testing environment in real-time. A HIL simulation is a type of simulation in which a real device or component is embedded in a virtual simulation environment. By combining real hardware and a virtual environment, complex systems can be tested. The HIL simulation technique enables developers to test the performance and reliability of the system without any safety risks. It is considered an important tool in the development process due to its ability to reduce costs and accelerate development time [3, 4, 5].

Another important challenge in the development of powertrain systems is ensuring functional safety according to ISO 26262. This international standard for functional safety of road vehicles outlines requirements for the safety of electrical and electronic systems in vehicles. The standard covers a range of requirements for the development, validation, and verification of safety-critical systems [6].

Fault Injection Testing (FIT) is an important aspect of functional safety recommended by the ISO 26262 as a method for evaluating the

reliability of safety systems. FIT is a method for simulating faults in a powertrain system to determine whether the system operates safely and reliably under all conditions. It involves deliberately introducing faults into the system to assess how the system responds to these faults [6, 7, 8]. This method is increasingly being used in the field of vehicle development. Therefore, FIT is an important tool for testing and validating electric vehicles [9, 10].

The current state of the art in the HIL field is represented by companies such as OPAL-RT and Typhoon HIL, which offer scalable and real-time capable HIL solutions based on FPGA technology for simulation in the field of electromobility [11]. These companies enable the simulation of power electronics and electrical components of electric vehicles, providing interfaces for the integration of real hardware. Companies like dSPACE and AVL SET also offer HIL solutions in the automotive sector. The combination presented in this work, involving real-time simulation of detailed electrical components of a complete electric vehicle on a Typhoon HIL device, coupled with the simulation of vehicle dynamics and environment in CarMaker, is entirely novel and provides a new level of simulation. Additionally, the combination with FIT introduces new possibilities in the field of vehicle validation. It is also important to consider the simulation accuracy of CarMaker, which has been examined in several studies and found to accurately represent reality [12].

This paper presents a co-simulation in which the powertrain of a battery electric vehicle with all its electrical components, including the high-voltage battery, the battery management system, the inverters and the motor models, is simulated on a real-time HIL system. This system is coupled with simulation software for virtual test drives [13]. The driving environment software simulates the vehicle body, the driving dynamics, the driver, the road and driving conditions such as snow. This connection of these two simulation environments makes it possible to test the entire vehicle behavior including detailed component models under different conditions.

The focus of the work is on fault injection testing, where faults are specifically introduced into the powertrain to observe the behavior of the vehicle model. Co-simulation can be used to test both the response at the powertrain level with all electrical components and the driving dynamic response of the vehicle on the road. This paper shows how such co-simulation can contribute to functional safety according to ISO 26262.

The present work introduces an original, new, and innovative approach through the development of a co-simulation between IPG CarMaker and Typhoon HIL. By combining these two components, entirely new possibilities emerge in real-time simulation of high-fidelity vehicle components such as inverters, electric motors, and batteries, integrated with the vehicle dynamics simulation in IPG CarMaker. Particularly in the field of functional safety and in conjunction with fault-injection testing, innovative pathways are demonstrated to gain new insights and address challenges in vehicle development.

At the beginning of this paper, the function and the individual components of the co-simulation are described. Then faults are presented, which are injected into the powertrain under different conditions. The reaction of the system to these is tested and analyzed. Finally, a statement about the function of the FIT according to ISO 26262 in this model is made and possible future applications and extensions are presented.

Co-Simulation Setup

The co-simulation addressed in this paper consists of two simulation environments. A real-time HIL604 simulator from Typhoon HIL with Typhoon HIL Control Center software simulates the electric powertrain and its detailed high-fidelity components.
The CarMaker software from IPG is used as the driving environment simulator, which runs on a host computer. Communication between both models is realized via Controller Area Network (CAN). To establish a CAN bus connection between the two components, a Peak CAN to USB adapter is used to connect the PC to the real-time simulator. In Figure 1, the setup of the co-simulation with the HIL604 and the PC is shown.

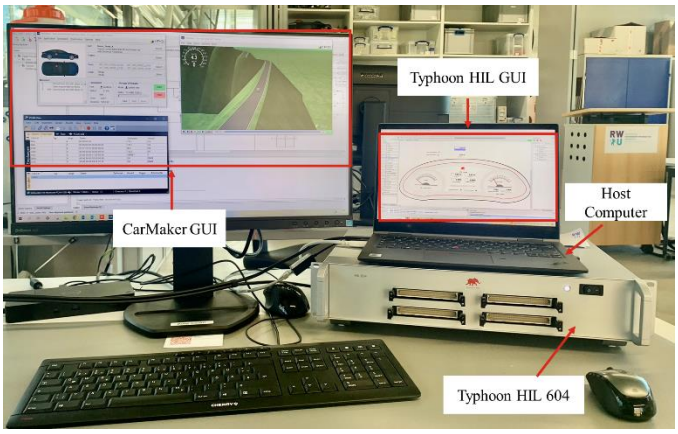

Figure 1. Co-Simulation hardware setup

The simulated vehicle model is a four-wheel drive battery electric vehicle, which is powered by one asynchronous motor per axle. The model vehicle is based on a Tesla Model X 100D. The collection of values and verification of the model are described in [13]. All powertrain components, such as electric motors, inverters, controller, battery, and battery management system, are simulated on the HIL. The road, the vehicle body, the driver, the resulting driving resistances and also the driving dynamics are simulated in the CarMaker simulation environment. By combining these simulation models, a vehicle simulation at system level with new possibilities is created. The specific models and their components will be described in more detail in the following chapters.
All important vehicle parameters as power, torque, speed, and battery information are listed in Table 1.

Table 1. Vehicle parameter

Max. motor power	193 kW
Recuperation motor power	30 kW
Max. motor torque	330 Nm
Recuperation motor torque	125 Nm
Max. vehicle speed	250 km/h
Battery capacity	103.55 kWh
Battery nominal voltage	398.4 V

Powertrain Model

Figure 2 shows the electric powertrain model running on the Typhoon HIL. It is a vehicle with all-wheel drive, equipped with one asynchronous motor per axle. The front and rear axle powertrain are identically designed. The electrical components of the powertrain model, which consists the two high-fidelity asynchronous motor models and two inverter models including LC-filters to smooth out the harmonics of the three-phase alternating current are shown. In addition, there is a detailed battery and BMS model which will be discussed in more detail in the next sections. Between the battery and inverter, there is a DC-link capacitor and the main contactor, as well as a pre-charge resistor to pre-charge the capacitor and limit the inrush current.

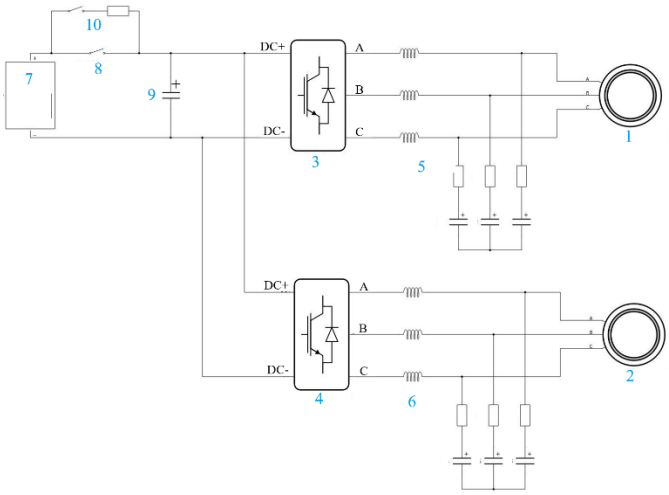

Figure 2. Components of the electric powertrain

1. Asynchronmotor front
2. Asynchronmotor rear
3. Three phase inverter front
4. Three phase inverter rear
5. LC-filter front
6. LC-filter rear
7. Battery
8. Main Contactor
9. DC-link Capacitor
10. Precharge resistor

Figure 2 shows the electrical components of the powertrain in a top level. The actual model also includes software components such as field-oriented controllers for the inverters, the BMS, and a CAN receiver and transceiver. Including those detailed models, the simulation time step is set to 1 µs on the HIL604 hardware.

Battery Model

The battery model is a 400 V lithium-ion battery system with a capacity of 103.55 kWh. The schematic layout of the battery is precisely shown in Figure 3. It can be seen that there are two strings, each consisting of three modules.

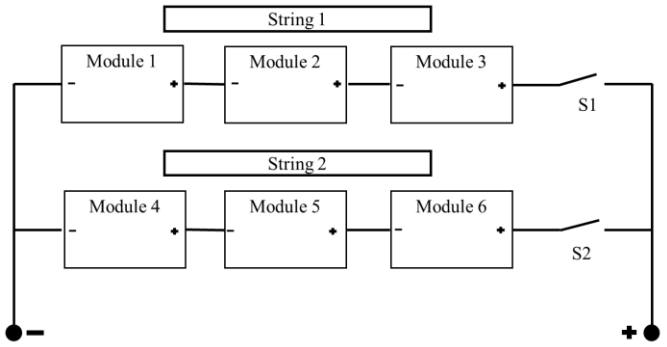

Figure 3. Schematic layout of the battery model

Each module consists of 32 cells in series and 9 cells in parallel, with each cell having a maximum voltage of 4.15 V and a maximum capacity of 14.44 Ah. A battery cell model is used, which is able to calculate the voltage, current, temperature, and state of charge of the cell, and consider how the internal resistance of the cell affects its operation [14].

To enable the calculations, vectors are given for the state of charge (SOC), temperature, open circuit voltage (OCV), internal resistor, coulombic efficiency, and total capacity. Look-up tables are then created from these values. Since there is insufficient information available for the original cells of the Tesla Model X 100D, the values of a fictitious 4.15 V lithium-ion cell are used instead. The following figures show the cell data. Figure 4 shows the OCV as a function of SOC. Figure 5 shows the internal resistance of a cell as a function of temperature.

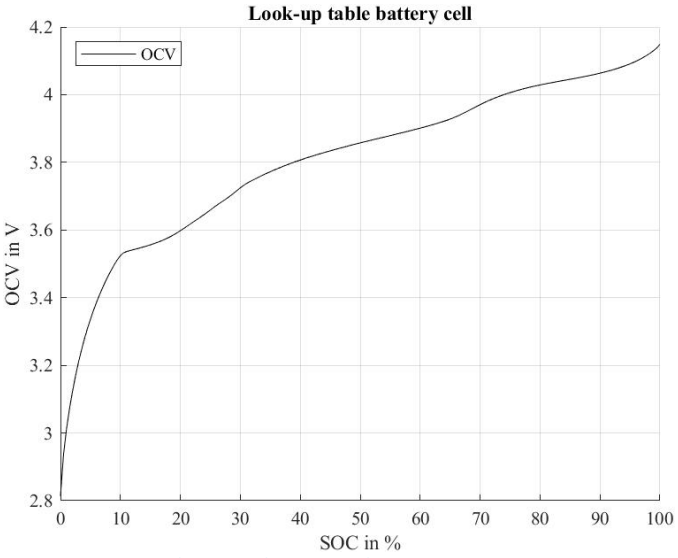

Figure 4. OCV as a function of the SOC of a single cell

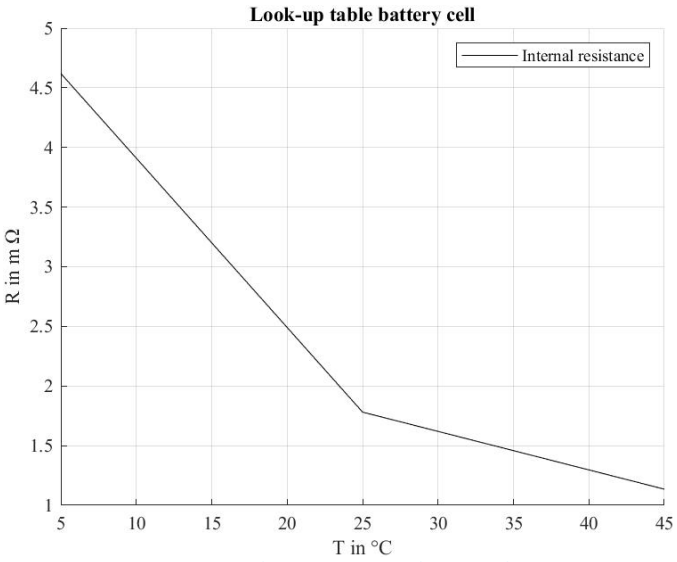

Figure 5. Internal resistance of a single cell as a function of temperature

The SOC of the cells is calculated using the Coulomb counting method according to the formula (1). Where Q is the total capacity of the battery, i is the cell current, and η is the Coulomb efficiency, which for simplicity is applied only when charging the cell. When discharging, the value of η is 1.

$$SOC(t) = \int \frac{i(t) * \eta(SOH, T)}{Q\ (SOH, T)} dt \quad (1)$$

Due to runtime limitations on the HIL side, it is not possible to simulate each cell individually. Therefore, one cell model is used for each module that represents a whole battery module. For this purpose, each value of the OCV and internal resistance vectors are multiplied by the number of cells connected in series. This results in a maximum voltage of 132.8 V per module with 32 cells in series.

To achieve the total battery capacity of 103.55 kWh, each module requires a capacity of 17.26 kWh. To achieve this with a cell with a maximum capacity of 14.44 Ah, nine cells need to be connected in parallel. The battery is thus a 32s9p system. This feature is integrated into the existing cell model. The parallel connection is modeled by dividing the cell current by the number of cells connected in parallel. It is assumed that all cells in a module have the same parameters.

In addition, the battery model includes switches S1 and S2 (see Figure 3), which allow to disconnect a battery string in case of a fault in one of the modules. Since both strings are connected in parallel, the vehicle still has a 400 V power supply even with one string disconnected. This makes it possible to isolate only the string where the fault occurs, without immediately opening the main contactor.

In module 1 and module 4, there is the possibility to modify only a single cell row. To make this possible, an additional cell model was integrated into each of these two modules, which simulates only one cell in series and nine cells in parallel. The second cell model in these modules now simulates 31 instead of 32 cells. So, the parameters of the total module remain the same as the others and still have 17.26 kWh and 132.8 V. This function was integrated for fault injection testing, to be able to introduce faults selectively only in one cell row and not the whole module.

Battery Management System

A BMS is an essential component of an electric vehicle. The main tasks of a BMS are to monitor and control battery parameters such as current, voltage, temperature, and cell state, to protect the battery against overcharging, deep discharge, overheating, short-circuit, and other malfunctions [5, 15]. In the powertrain model of the co-simulation, a BMS is also integrated. This has the following functions:

- Pre-charging: The BMS controls the starting process of the vehicle. When the user initiates the start, the BMS pre-charges the DC-link capacitor via a pre-charging resistor and then closes the main contactor. Thus, the battery is connected to the powertrain, and the inverters are enabled.
- Temperature monitoring: The BMS monitors the temperatures of all cells. Here a minimum temperature of -15 °C and a maximum temperature of 50 °C are stored in the system. If a cell exceeds these limits, the BMS immediately responds and disconnects the string in which the faulty cell is located.
- Voltage monitoring: All cell voltages are monitored by the BMS. Minimum and maximum cell voltages can be variably adjusted. If one of these values is exceeded, the BMS responds by opening the main contactor.
- Short-circuit detection: To detect a possible short circuit in the powertrain system, the total current is continuously measured. If this current exceeds the maximum limit, the BMS assumes that there is a short circuit in the system and opens the main contactor for safety. In vehicles, the control can be supported using the continuous measured insulation resistance of the high-voltage system.
- Discharge protection: If the battery is discharged to almost 0% SOC, the cell voltages decrease strongly, and the BMS opens the main contactor to protect the cells from deep discharge.
- Derating function: The BMS also plays an important role in reducing the power flow and relieving the battery. In the event of a single-string operation, which serves as an emergency mode, the battery capacity is halved, resulting in higher stress on the remaining cells. For this reason, driving performance is greatly restricted. Once the BMS executes a single-string operation due to an fault, it sends information to the controllers, which then reduce vehicle power.

As the balancing function is not relevant for fault injection, it was dispensed with in this case. Additionally, in real-world operation, it would make sense to introduce far more derating functions to also consider the C-rate of the cells. In the case of this model, the performance of the cells is actually not limited.

Inverter Model

To convert the battery's direct current for the alternating current motors, an inverter is used for each drive unit. These are three-phase voltage source inverters that are frequently used in electromobility [16].
Here, a model from the Typhoon HIL library is used [17]. The model, as shown in Figure 6, consists of six insulated gate bipolar transistors (IGBTs), which are controlled by a space vector pulse width modulation (SVPWM) from the controller so that the switches S1 and S2 of the three phases A, B, and C are switched in a certain pattern, resulting in a three-phase alternating current. This is then smoothed by the LC-filter (see Figure 2). With this alternating current (AC), the asynchronous motor can be controlled. The carrier frequency of the inverter in this powertrain is 20 kHz.

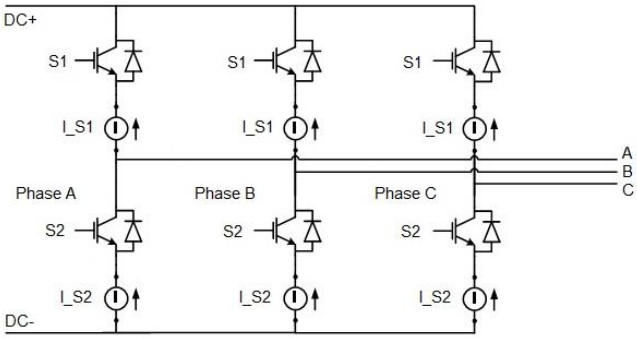

Figure 6. Layout of the 3-phase inverter model [15]

The DC-link capacitor (See Figure 2) ensures that the ripple current and voltage generated by the switching processes are reduced, thereby providing a more constant intermediate circuit voltage.

Controller

The inverter is controlled by an Indirect Field-Oriented Controller (IFOC), which also runs on the HIL simulator. IFOC is a control strategy for electric machines that enables precise control of torque and speed. The field-oriented control is based on the principle of field orientation, where the magnetic fields of the machine are divided into two components, a torque-producing and a flux-producing component. The controller determines the instantaneous values of these components and calculates the necessary control signals for the inverter to regulate the speed and torque of the machine. The IFOC is an indirect field orientation, where the flux in the machine is estimated and not directly measured. [18]

As input variables the three-phase currents, which are measured in the model, the current speed and torque, as well as the load requirement from CarMaker, are used [13]. Based on these input variables and the motor parameters, this controller regulates the SVPWM signal to control the inverter [19].

In Figure 7, all input and output variables of the controller are shown. On the left side, the measured phase currents, the speed sent by CarMaker, the current motor torque, and the accelerator pedal position are shown as input variables. On the right side, the PWM reference signals ma, mb, and mc for controlling the inverter are shown as output variables.

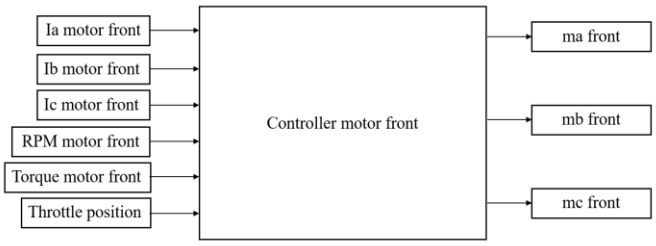

Figure 7. Input and output variables of the indirect field-oriented controller

The aim is to run the control system in future projects with real control units (Controller-HIL).

Asynchronous Motor Model

The electric motors in use are two asynchronous machines which are exactly identical in design. Each motor drives an axis and has a maximum power output of 193 kW. The maximum recuperation power is defined at 30 kW based on the data of the test vehicle. The parameterization of the electric motors is carried out in [13] and is based on a motor with comparable requirements, due to the lack of information on the motor data of the Tesla Model X. The model allows for a detailed representation of motor dynamics. It takes into account, the influence of rotor and stator losses, as well as the effects of magnetic saturation phenomena [20].

Vehicle Model CarMaker

CarMaker is a simulation software that enables the representation of virtual driving scenarios, including the simulation of the driving dynamics of a real vehicle and its environment. In addition, it allows for virtual driving tests to be performed, enabling the testing of a vehicle's dynamic response in various situations. For co-simulation, CarMaker simulates the road, the vehicle body, the driving resistances, and the driver. The IPG Movie function allows for the visualization of the vehicle's behavior on the road. Figure 8 shows the test vehicle during a test drive on a synthetic road with snow on the surface in IPG Movie. [21]

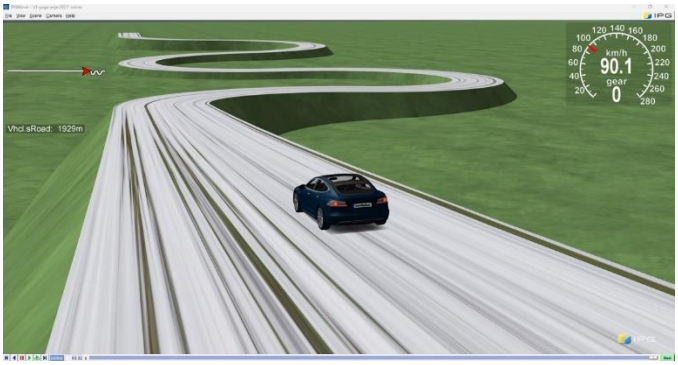

Figure 8. Test vehicle on snowy road using the CarMaker IPG Movie function

In CarMaker, an electrical powertrain model with two electric machines is used. Since the electric powertrain runs externally on the real-time simulator, replacement models written for the motors are used from [13]. These models include communication with the real-time simulator and send speed and load requirements to the HIL. In addition, a replacement model for the battery control unit is implemented since the battery and BMS including SOC calculation, also runs on the HIL and should be transferred to CarMaker.

Furthermore, in CarMaker, all important data about the vehicle body is provided. This includes, among other things, the vehicle weight, frontal area, and length of the vehicle [22]. The tire model is also selected and defined in CarMaker. Based on this data, CarMaker can calculate the driving resistances. Important information about the vehicle body and tires are listed in Table 2. The parameterization of the vehicle body was carried out in [13] and is also based on the Tesla Model X 100D.

Table 2. Vehicle body parameter

Vehicle mass	2487.14 kg
Vehicle front area	2.59 m²
Vehicle length	5.037 m
Front tires data	265 35R22
Rear tires data	285 35R22

Additionally, the vehicle is loaded with a person of 70 kg on the driver's seat.

Test Scenario

To perform the fault injections, a suitable synthetic test track is modeled in CarMaker. This is a track with a length of 2380 m. Figure 9 shows the track profile with the labeling of the track sections. Section 1 is a 500 m flat track, followed by a positive 12 % incline in section 2, then another 500 m straight in section 3. Section 4 goes down with a negative 12 % incline. Section 5 begins at 2000 meters. Here, there are three 180-degree curves on a flat surface with a radius of 40 m.

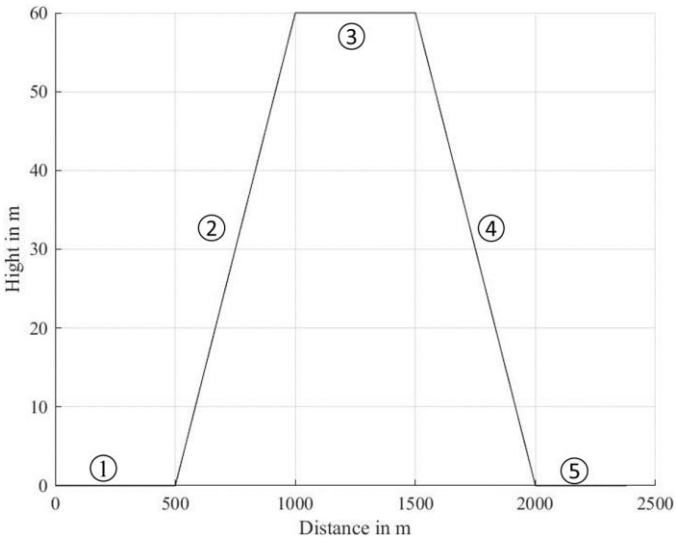

Figure 9. Test scenario track profile with labelled track sections

Figure 10 shows an overhead view of the track. Here, the straight street from section 1 to 4 can be seen, and on the right the three 180° curves of section five are shown.

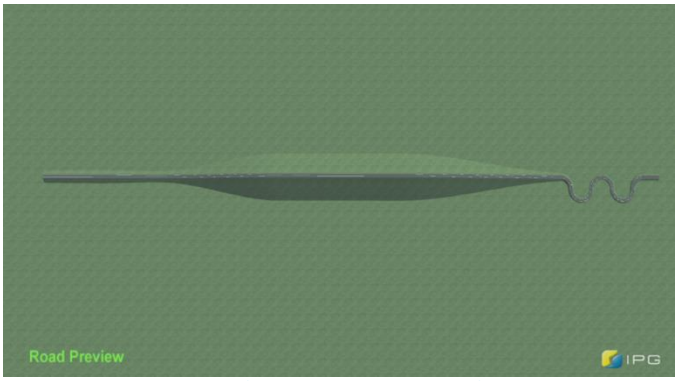

Figure 10. Overhead view of the test scenario track profile

For this route, two states are implemented. One with dry asphalt, where the friction coefficient is 1, and one with light snow on the street, where the friction coefficient is 0.35.

CAN Communication

As previously mentioned, both simulation environments communicate via CAN. Table 3 shows all CAN messages sent from CarMaker to Typhoon HIL. Table 4 displays all the signals sent from the powertrain model on the HIL to the CarMaker model. In order to be able to control the motors in the powertrain model, the current motor speeds as well as the load request in the form of the accelerator pedal position is sent from CarMaker to Typhoon. The HIL calculates the motor torques and sends them back to CarMaker.
For debugging purposes, CarMaker also sends the current torque and Typhoon the motor speeds. This is not required for the normal function of the co-simulation. In addition, vehicle speed, which results from the travelled distance and brake pedal position are send from CarMaker for visualization purposes. Furthermore, the SOC of the high-voltage battery is transmitted from Typhoon to CarMaker. CarMaker uses a baud rate of 1 Mbits/s. To reduce bus load, the values are only transmitted every 10th computation cycle. The HIL sends the data every 2 ms.

Table 3. CAN communication from CarMaker to Typhoon HIL

ID	Bit 0-32	Bit 32-64
101	Traveled distance	-
102	Throttle	Brake
201	Torque front	Motor speed front
301	Torque rear	Motor speed rear

Table 4. CAN communication from Typhoon HIL to CarMaker

ID	Bit 0-32	Bit 32-64
701	Motor speed front	Torque front
801	Motor speed rear	Torque rear
501	SOC HV-battery	-

Through the CAN communication, both simulation environments are connected and the co-simulation is operational.

ISO 26262

The ISO 26262 is a standard that defines requirements for the functionality and safety of safety-critical systems in the automotive industry. The standard covers the entire development process of safety-critical systems and sets requirements for each phase of the development process. These include, for example, the concept phase, hardware and software development, and system-level development. Testing and validating safety requirements plays a significant role in all phases. With the trend of increasing technological complexity, the risks from systematic faults and random hardware failures are increasing. The goal of ISO 26262 is to mitigate these risks through appropriate requirements and procedures. [6]

Fault injection testing also plays an important role in this standard. It is used in the area of system-level development in the field of system testing and safety validation. The Standard describes fault injection testing as a systematic method of introducing faults into the system and evaluating the resulting effects. [9]

Fault Cases

To apply the fault injection testing method to the co-simulation, various options were embedded into the powertrain model to integrate faults. Here, the faults were deliberately distributed among the different powertrain components in order to observe various reactions of the vehicle.

In the battery, there is the possibility to generate an over-temperature in one cell each in module 1 and module 4 (see Figure 3). The BMS continuously monitors all cells for current, voltage, and temperature, therefore a reaction of the BMS is expected. Since the fault occurs only in one battery string, only the faulty string should be disconnected. If the cell fault occurs in module 4, the BMS should open contactor S2. Thus, the faulty string is disconnected and a single-string operation is generated. In addition, the vehicle power should be limited by the Bus.

In the inverter, there is the possibility to introduce a shoot-through. This is a state where the IGBTs of S1 and S2 (see Figure 6) of one phase are closed simultaneously [23]. This creates a DC short circuit. This short circuit should also be detected by the BMS and the main contactor (see Figure 2) should be opened as quickly as possible in response to protect the battery.

Another fault case is excessive recuperation on only one axle. Recuperation is the regenerative operation of the electric motor. Here, the kinetic energy of a rolling vehicle is converted back into electrical energy, slowing down the vehicle. The standard recuperation of the vehicle is designed for a maximum of 30 kW per motor. In this fault case, the rear axle recuperates with 75 kW and the front axle does not recuperate at all. This fault is introduced in the controllers.

The faults are introduced at different points and under different conditions of the test track. In Table 5, all faults with the track positions (see Figure 9) at which they are occur, the expected reaction, and road conditions are listed again.

Table 5. Fault cases for fault injection including conditions and expected reaction

Fault	Expected Reaction	Position	Condition
Hot battery cell	Single string drive & derating	1	Dry
Shoot-through inverter	Open main contactor	2	Dry
Recuperation fault	Changed driving behavior	4/5	Snow

In all fault cases, the influence on the electrical components in the powertrain as well as on the driving dynamics can be analyzed through co-simulation. On the HIL platform, it is possible to retrieve data from the electrical powertrain, such as DC side voltages and currents at the cell and overall battery level, as well as at the intermediate circuit capacitor. Additionally, phase currents and voltages on the AC side can be measured. Furthermore, all motor data like torque and motor speeds are captured. The signals from the IGBTs in the inverters, contactor switching signals, and signals from the BMS are also logged. Additionally, temperature values of the battery cells and the inverter can also be captured. On the CarMaker side, the vehicle dynamics data are recorded. Here, for example data like vehicle speed, acceleration values in different axes, tire slip, yaw angle, yaw acceleration and yaw rate, as well as steering, braking, and throttle values are captured.

Fault Injection Testing

All fault cases are incorporated into the co-simulation, and the electrical behavior of the powertrain, as well as the driving dynamics of the vehicle on the road, are documented and evaluated. In the following sections, the vehicle's response to the various fault injections will be analyzed.

Battery Fault Injection

In this case, the cell temperature of a cell in battery module 1 is increased from 25 °C to 60 °C. This can also be seen in Figure 11 in Section 1. Since the maximum temperature is defined as 50 °C, the BMS immediately reacts and disconnects the battery module with the faulty cell. This is shown in the second graph, which shows that switch S2 (blue) remains in state 1, which means closed, and switch S1 (black) immediately switches to state 0 (open) when the maximum temperature is exceeded. Single-string operation is only an emergency function to, for example, drive to the nearest workshop. To protect the battery, which now only has half of its capacity, the power is limited to 10 kW per motor. This derating behavior is shown in Section three of the figure. This power reduction can also be observed in the vehicle velocity in Section four. Here, the vehicle gradually slows down as the fault is performed on an uphill climb.

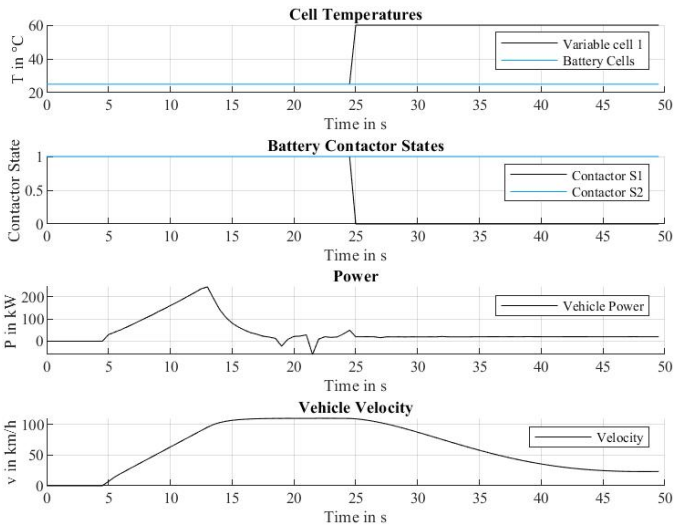

Figure 11. Graph of cell temperature, contactor states, power and velocity when a cell fault is introduced

Inverter Fault Injection

In this case, a shoot-through is introduced on Phase A in the inverter. For this purpose, an IGBT (see Figure 6) is controlled independently from the SVPWM signal and becomes conductive. Once the second IGBT on the phase closes, DC+ and DC- are connected, causing a DC short circuit. This short circuit is immediately detected by the BMS through the increased current, which opens the main contactor and disconnects the high-voltage battery.

In Figure 12 in section one, the battery current I is shown. The figure shows the peak value of the battery current at 28 seconds. This shows the moment of DC short circuit. The switching behavior of the main contactor is shown in section two in black. The main contactor is closing at start after pre-charging the capacitor. During normal driving it is on state 1 (closed). At the moment the battery current increases the overcurrent flag (blue) in section two is raised by the BMS and the main contactor switches to state 0 (open).

In section three, the immediate decrease in power can be observed. The negative peak at 30 seconds, even though the contactor is open, can be explained by the energy charging the DC link capacitor.
In section four of the graph, the speed of the vehicle can be observed. It decreases continuously as the main contactor opens and the power decreases. Since the fault is introduced at the beginning of the first uphill section, the vehicle rolls out relatively quickly.

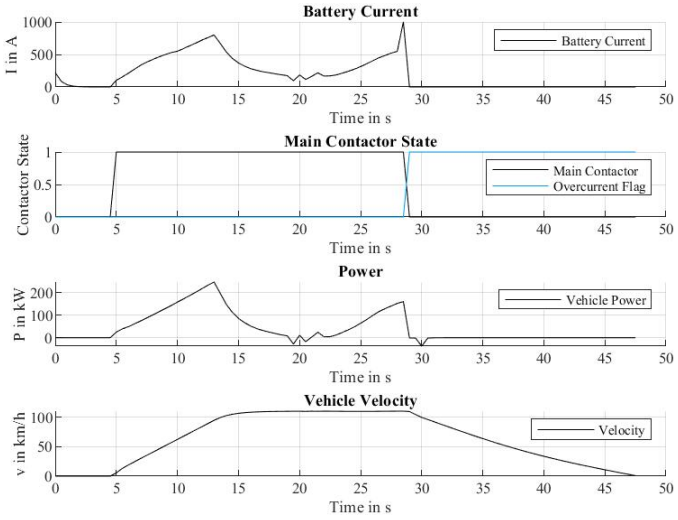

Figure 12. Graph of battery current, contactor states, power and velocity when a inverter fault is introduced

Recuperation Fault Injection

This fault is attributed to a problem with the controller, which is regulating regenerative braking incorrectly. As a result, the vehicle is not regenerating with the standard power of 30 kW per axle, but with an increased regenerative power of 75 kW at the rear axle. Regenerative braking is completely disabled at the front axle. The purpose of introducing this fault is to illustrate the effects of regenerative braking on a snowy road, where the friction coefficient of the road is 0.35. This fault is introduced from the beginning of the drive, but it only becomes evident at the end of section 4 of the track (as shown in Figure 9), when the vehicle begins regenerating at full power as it exits the negative slope and enters the 180-degree turn.

Figure 13 shows the power of the vehicle, where the negative power corresponds to regenerative braking power. The results are consistent with the characteristics of the fault, as the power of the front motor (in black) never goes into the negative range, while the rear motor regenerates with a power up to -75 kW.

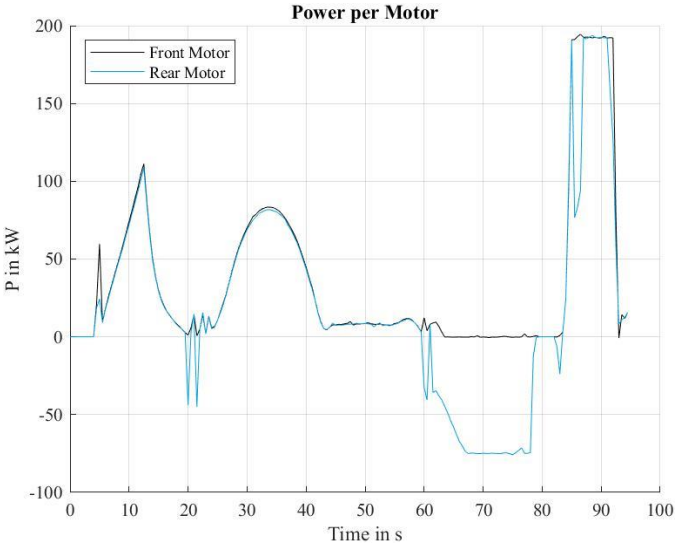

Figure 13. Graph of power per motor during recuperation fault injection

The strong regenerative braking on a single axle can also be observed in the vehicle's driving dynamics. Figure 14 shows the dynamic vehicle's behavior graphically. At point a, the vehicle enters the curve downhill from the negative slope. Already at the entry of the curve in point b, the vehicle begins to experience slight oversteer, and the rear end continues to slide out from point c to e until the vehicle finally comes to a stop at point f.

Figure 14. Vehicle dynamics during recuperation fault injection on snowy road

The behavior of the vehicle can also be observed in Figure 15. The first section shows the yaw angle of the vehicle. The yaw angle is the angle between the x-axis of the car and the x-axis of the earth-fixed system [22]. A positive rotation around the z-axis results in a positive value. The blue line shows the yaw angle during normal driving without any fault. The black line shows the driving with the fault injection of the recuperation fault. Here it can be seen that the vehicle enters the curve as in normal driving, but the yaw angle increases as the vehicle loses control.

In the second graph of Figure 15, the lateral acceleration a_y of the vehicle is shown. Again, the blue line represents the measurement during normal driving without any fault, and the black line represents the drive with fault injection of the recuperation fault. The lateral acceleration represents the component of the acceleration in the y-direction. In this graph, the point at which the vehicle loses control is clearly visible, with the lateral acceleration component exceeding the negative range.

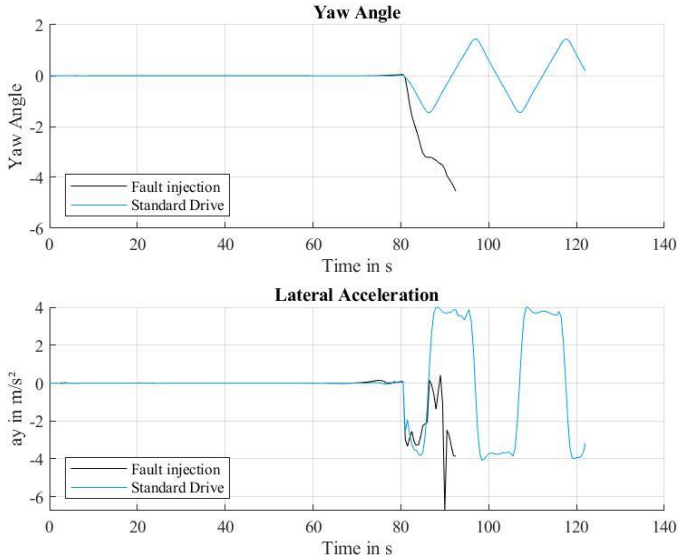

Figure 15. Graph of yaw angle and lateral acceleration during recuperation fault injection and normal drive without faults

Discussion

In summary, it can be stated that this co-simulation is a very valuable tool in the development of electric powertrains. By using fault injection tests, co-simulation can be utilized for system testing and safety validation at the system level, making a significant contribution to functional safety of safety-critical systems in the automotive industry according to ISO 26262.

The functionality and versatility of the system are demonstrated by the three fault injection tests in this work. It is evident that there are broad possibilities for introducing faults, and the data evaluation possibilities are also diverse.

Faults can be introduced as needed in the powertrain and tested under various driving routes and environmental conditions. Additionally, this work shows that the analysis of faults is possible on all levels. Thus, the electrical behavior of individual components of the powertrain can be observed, but also, the dynamic behavior of the vehicle at the system level can be analyzed.

The co-simulation approach enables the discovery and testing of critical edge cases and allows for the visualization of interactions between all system components at the system level.

Currently, the limitations of the system are restricted to soft real-time. To run the model in hard real-time, it is necessary to execute CarMaker on a HIL system instead of a host PC. There is already the IPG Xpack available, which is a HIL solution for real-time simulation of CarMaker with hardware interfaces. This approach can be considered in future applications. Additionally, it would be beneficial to increase the limits of the bus load to enable more frequent transmissions between HIL and CarMaker.

The main objective of this study is to effectively test the integration and compatibility of the two systems. In future applications, the maneuvers and models to be performed should be verified. A current limitation is that the vehicle in the simulation does not include driver assistance and vehicle safety systems such as emergency braking assist, ABS, and ESP. This limitation was consciously accepted for the initial testing phase. In future investigations, it is planned to implement the software on a control unit, such as an ABS controller, in the form of Controller in the Loop, to further expand the capabilities of the HIL setup.

The co-simulation creates additional possibilities in the field of vehicle development. For example, by integrating efficiency maps, temperature and loss models, it can be used for realistic energy consumption measurements. This would also enable the optimization of temperature behavior and efficiency of individual components for specific routes.

Looking towards the future, it should be noted that such co-simulation, including fault injection testing, can also play an important role in the development of autonomous driving systems. It can be used to address the challenges associated with the development and testing of functions and safety for autonomous vehicles.

The toolchain enables multiple development partners to simultaneously test functions or errors by combining high-fidelity vehicle simulations. This includes the joint examination of safety systems such as emergency braking assist in combination with inverter software and sensors. This work stands out due to its innovative approaches, novel integration of simulation components, and its contribution to the development of new methods and opportunities. An outlook for future work involves expanding the toolchain to incorporate additional components and functions, as well as extending its application to different vehicle types and scenarios.

References

1. Hansmann, J., Millitzer, J., Rieß, S. and Balzer, L., “Symbiose virtueller und experimenteller Methoden für effizienteres Testen und Entwickeln, ” Liebl, J. Experten-Forum Powertrain: Simulation und Test 2019 Proceedings, 2020, doi:10.1007/978-3-658-28707-8_4.
2. Santos, J. and Vieira, G., de Oliveira Vasconcelos, F., Silva, E. et al., “Virtualization X Real Component: The Advantages of System Modeling on the Automotive Development Process,” SAE Technical Paper 2017-36-0229, 2017, doi:10.4271/2017-36-0229.
3. P, A., M, V., Vavilapalli, K. and NK, J., “HiL Testing of Automotive Transients in Electric Vehicle,” SAE Technical Paper 2022-28-0378, 2022, doi:10.4271/2022-28-0378.
4. Pintaric, I., Costa, S., Genic, A., Zuber, D. et al. “Flexible HiL Interface Implementation for Automotive XiL Testing,” IEEE Vehicle Power and Propulsion Conference (VPPC), 2021, doi:10.1109/VPPC53923.2021.9699257.
5. Schärtel, L., Reick, B., Pfeil, M. and Stetter, L., “Analysis and Synthesis of Architectures for Automotive Battery Management Systems,” MDPI Applied Sciences 12, no. 21: 10756, 2022, doi:10.3390/app122110756.
6. ISO 26262-1:2028(E), “Road vehicles - Functional safety,” Part 1: Vocabulary, 2018.
7. Reyes, V., “Virtualized Fault Injection Methods in the Context of the ISO 26262 Standard, ” SAE Int. J. Passeng. Cars - Electron. Electr. Syst. 5(1):9-16, 2012, doi:10.4271/2012-01-0001.
8. Ringdorfer, M., Griessnig, G., Draxler, P. and Schnellbach, A. “A Systematical Approach for “System Item Integration and Testing” in Context of ISO 26262,” Communications in Computer and Information Science, vol 1251. Springer, Cham., 2020, doi:10.1007/978-3-030-56441-4_42.
9. ISO 26262-1:2028(E), “Road vehicles - Functional safety,” Part Part 4: Product development at the system level, 2018.
10. Holzmann, H., Landersheim, V., Piram, U., Bartolozzi, et al., “Fault Injection in Actuator Models for Testing of Automated Driving Functions,” MDPI Vehicles 5, no. 1: 94-110, 2023, doi:10.3390/vehicles5010006.
11. Jia, X., Adhikari, M. P., and Vanfretti, L.,“Real-Time Simulation Models for Photovoltaic Cells and Arrays in Opal-RT and Typhoon-HIL, ” IEEE Power & Energy Society General Meeting (PESGM), Montreal, QC, Canada, 2020, doi:10.1109/PESGM41954.2020.9282171.
12. Schick, B., Henning, J., Wurster, U. and Klein-Ridder, B., “ Simulation methods to evaluate and verify functions, quality, and safety of driver assistance systems in the continuous MIL, SIL, and HIL process, ” 3. Tagung Aktive Sicherheit durch Fahrerassistenz, 2008.
13. Riedel, J., “Aufbau und Implementierung einer echtzeitfähigen SiL Co-Simulation eines batterieelektrischen Fahrzeugmodells,” Master Thesis HTW Saar, 2022.
14. Typhoon HIL, Software Manual, “Battery Cell, ” https://www.typhoon-hil.com/documentation/typhoon-hil-software-manual/References/battery_cell.html.
15. Gabbar, H., Othman, A. and Abdussami, M., “Review of Battery Management Systems (BMS) Development and Industrial Standards,” MDPI Technologies 9, no. 2: 28, 2021, doi:10.3390/technologies9020028.
16. Reimers, J., Dorn-Gomba, L., Mak, C. and Emadi, A., “Automotive Traction Inverters: Current Status and Future Trends,” IEEE Transactions on Vehicular Technology, vol. 68, no. 4, pp. 3337-3350, 2019, doi:10.1109/TVT.2019.2897899.
17. Typhoon HIL, Software Manual, “Three Phase Inverter,” https://www.typhoon-hil.com/documentation/typhoon-hil-software-manual/References/three-phase_two-level_inverter_rectifier.html?hl=inverter
18. Schröder, D. and Böcker, J., “Elektrische Antriebe – Regelung von Antriebssystemen,” Springer Vieweg Berlin, 2021, doi:10.1007/978-3-662-62700-6.
19. Zhang, B. and Qiu, D., “m-Mode SVPWM Technique for Power Converters,” Springer Singapore, 2019, doi:10.1007/978-981-13-1382-0.
20. Typhoon HIL, Software Manual, “Three Phase Squirrel Cage Induction Machine,” https://www.typhoon-hil.com/documentation/typhoon-hil-software-manual/References/three_phase_squirrel_cage_induction_machine.html
21. IPG Automotive Group, “CarMaker User’s Guide Version 11.0.1,” 2022.
22. IPG Automotive Group, “CarMaker Reference Manual Version 11.0.1. 3.,” 2022.
23. Hasegawa, K., Abe, S., Tsukuda, M., Omura, I. et al., “Shoot-through protection for an inverter consisting of the next-generation IGBTs with gate impedance reduction,” Microelectronics Reliability Volume 114 113765, 2020, doi:10.1016/j.microrel.2020.113765.

Contact Information

Anja Konzept: konzepta@rwu.de

Definitions/Abbreviations

AC	Alternating Cuurrent
BEV	Battery Electric Vehicle
BMS	Battery Management System
CAN	Controller Area Network
Co-Simulation	Cooperative Simulation
DC	Direct Current
FIT	Fault Injection Testing
HIL	Hardware in the Loop
IFOC	Indirect Field Oriented Control
IGBT	Insulated-Gate Bipolar Transistor
OCV	Open Circuit Voltage
PWM	Pulse Width Modulation

SOC	State of Charge
SVPWM	Space Vector Pulse Width Modulation

© 2023 SAE International and SAE Naples Section. All rights reserved. No part of this publication may be reproduced, stored in a retrieval system, or transmitted, in any form or by any means, electronic, mechanical, photocopying, recording, or otherwise, without the prior written permission of SAE International.

Positions and opinions advanced in this work are those of the author(s) and not necessarily those of SAE International. Responsibility for the content of the work lies solely with the author(s).

ISSN 0148-7191
https://saemobilus.sae.org/content/2023-24-0181